ELSEVIER

Journal of Chromatography A, 806 (1998) 293–303

JOURNAL OF CHROMATOGRAPHY A

Gas chromatographic determination of binary adsorption isotherms

F. Roubani-Kalantzopoulou

Department of Chemical Engineering, National Technical University of Athens, 15780 Zografou, Greece

Received 5 August 1997; received in revised form 15 January 1998; accepted 19 January 1998

Abstract

Reversed-flow gas chromatography is a dynamic method useful for measuring adsorption isotherms at low concentrations. This method based on the mass-balance equations is useful for evaluating the adsorption isotherms because it gives model-independent results. The method is described and evaluated for the determination of the adsorption isotherms of two components in gas–solid systems. The following adsorbents were included in the study: iron oxide, zinc oxide, chromium oxide, lead oxide and titanium oxide. The adsorption of two significant aromatic hydrocarbons (benzene and toluene) was investigated in the presence of an inorganic gas (nitrogen dioxide). © 1998 Elsevier Science B.V.

Keywords: Adsorption isotherms; Inorganic oxides; Nitrogen dioxide; Benzene; Toluene

1. Introduction

Gas chromatography (GC) in contrast to static methods is of considerable interest for studying adsorption at finite surface coverages, because it readily allows measurements of over a wide range of temperatures [1]. This technique provides a means to determine the adsorption isotherms from which the surface area, porosity and surface energy [2,3] are determined. When adsorption takes place at finite surface coverages the isotherms are generally nonlinear and hence retention volumes are dependent upon the adsorbate concentration in the gas phase. In addition, a nonlinear isotherm results in asymmetrical peaks, the shape of which and the retention time being dependent on the volume injected.

The majority of papers devoted to single-gas adsorption assumed that the surface of the adsorbent is homogeneous; however single-gas adsorption systems with adsorbate molecules of complex chemical structure and adsorbents of complex chemical composition and porous structure cannot be described by means of equations derived for homogeneous surfaces [4]. Thus for these more complex systems, surface heterogeneity plays an important role and must be taken into account in the physicochemical interpretation of the adsorption process [5]. Various forms of perturbation chromatography have been used to measure pure-component isotherms and in a few cases even binary isotherms.

Gas–solid equilibrium isotherms of binary and more complex systems are of significant theoretical and practical interest. However, the experimental difficulties for complex systems have led to limited data available compared to the immense amount of information data and models available for single-component adsorption systems [6].

In this paper binary gas–solid experimental adsorption isotherms are presented using the technique and the methodology of the reversed-flow GC (RF-GC). This method is a well known perturbation chromatographic one combining simplicity with ac-

0021-9673/98/$19.00
PII S0021-9673(98)00058-2

curacy [7,8]; used recently in studying physicochemical constants in homogeneous gas phases [9,10] and as well as in heterogeneous ones [11–14].

2. Experimental

2.1. Materials

The adsorbates used were: benzene, toluene and nitrogen dioxide and were employed without further purification. Toluene was a Mallinckrodt analytical reagent and benzene especially for chromatography laboratory reagent from BDH (Poole, UK), while the nitrogen dioxide was from AirLiquide (Athens, Greece). The inorganic oxides: PbO, Fe_2O_3, TiO_2, Cr_2O_3 and ZnO were E. Merck (Darmstadt, Germany) analytical-reagent grade products, used as received.

Ultra-high-purity nitrogen was used as carrier gas.

2.2. Apparatus

Chromatographic measurements were carried out with a Shimazu (Duisburg, Germany) gas chromatograph, model 8A with a flame ionization detector. The experimental arrangement was analogous to that used in Ref. [13], with some modifications. Here the L_1 section (20.5–23.4 cm) was empty of any solid material, while the L_2 (4.0–5.0 cm) contained the solid bed. Both sections, L_1 and L_2, were of Pyrex glass of an I.D. 3.5 mm. The sampling column $l'+l$ (40 cm+40 cm) was of stainless steel chromatographic tube of 4.0 mm I.D. (cf. Fig. 1).

2.3. Procedure

Adsorbents were packed in columns made from Pyrex glass. Before the adsorption experiments, the column with the adsorbate was conditioned at 473 K for 24 h under a flow of nitrogen, followed every time by the adjustment of the working temperature (363.2 K for benzene and 393.2 K for toluene). The flow-rate measured at the outlet of the column was 26 ml min^{-1}.

A small quantity of liquid benzene (4.0 μl) or toluene (4.7 μl) was injected through the end of column L_2 with 0.2 ml of gaseous nitrogen dioxide at atmospheric pressure, and, after the appearance of the continuously rising concentration–time curve, the reversing procedure for the nitrogen carrier gas flow started, each reversal lasting always 10 s. This is

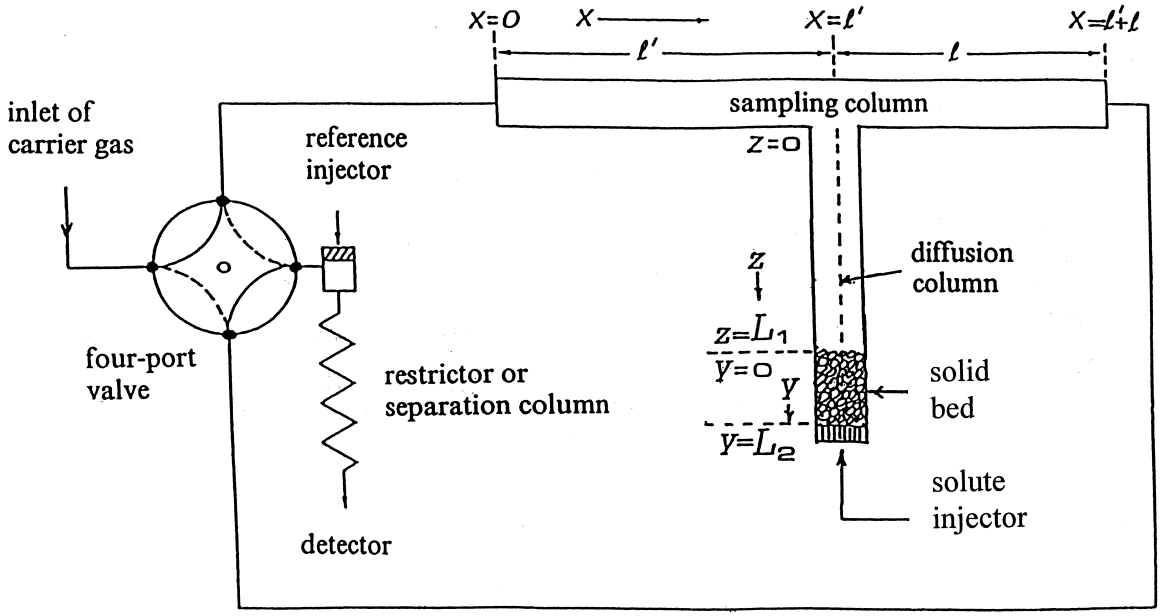

Fig. 1. The experimental set-up for studying binary adsorption isotherms.

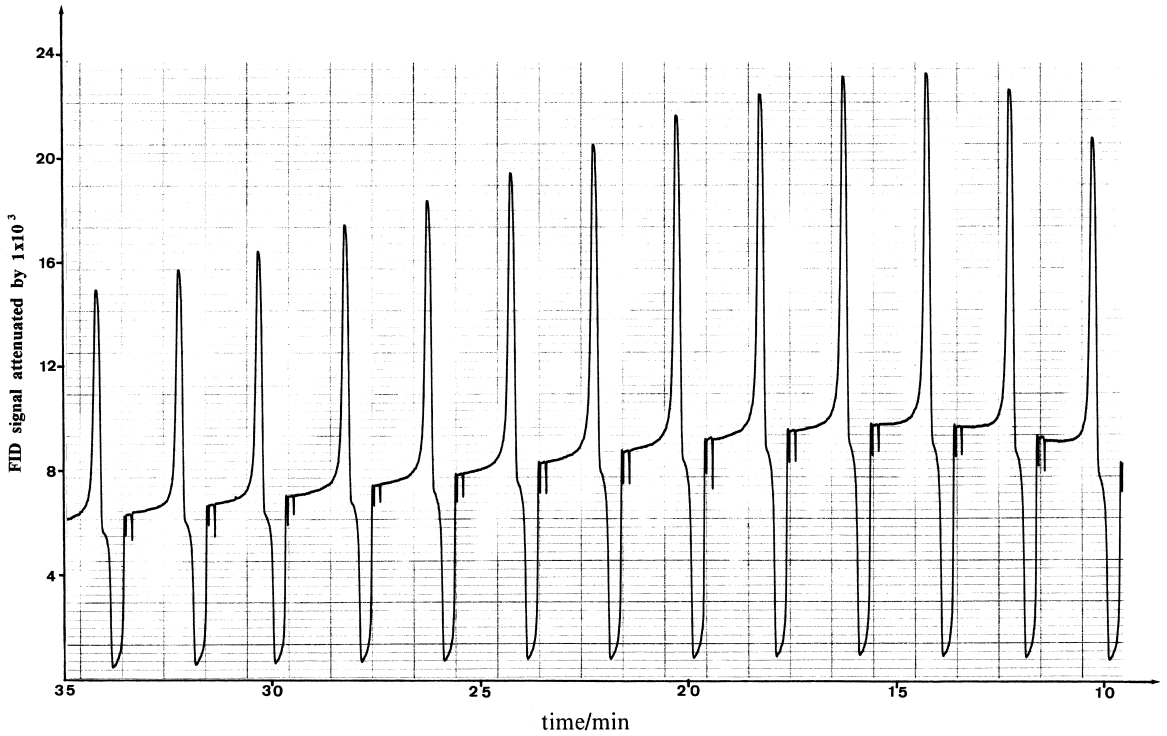

Fig. 2. Sample peaks of C_6H_6–NO_2 binary gaseous system on iron oxide at 363.2 K.

shorter than the gas hold-up time in the section l and l' of the sampling column.

The narrow fairly symmetrical sample peaks created by the flow reversals were recorded and their height was printed as a function of time t. This was done first for the aromatic compound only and secondly for the binary system. An example of the chromatograms resulting from the repeated flow reversals is shown in Fig. 2. More details about the experimental technique can be found elsewhere [8].

The external porosity and the specific surface area of the solids were taken from previous works [12,13]. It should be emphasized that these materials are essentially rather nonporous, which minimizes the problems of intraparticle diffusion. For reasons of convenience to the reader the values of these basic parameters are presented in Table 1.

Table 1
External porosity (ε) and specific surface area (SSA) of the five solids used

Solid	ε	SSA/cm^2 g^{-1}
ZnO	0.3840	17316
Cr_2O_3	0.7252	33400
Fe_2O_3	0.7988	23400
PbO	0.5551	300
TiO_2	0.5459	31100

3. Calculations

A brief outline of the theory underlying binary adsorption on solids is given. The simultaneous adsorption of binary gases on different adsorbents has been determined using the recently published model [12,15].

Four basic equations are mentioned.

First, the local adsorption isotherm of the gaseous analyte being studied:

$$c_s^* = \frac{m_s}{a_s}\,\delta(y - L_2) + \frac{a_y}{a_s}\,k_1 \int_0^t c_y(\tau)\mathrm{d}\tau \qquad (1)$$

Second, the mass balance equation for the analyte in the gaseous region z of the diffusion column:

$$\frac{\partial c_z}{\partial t} = D_1 \frac{\partial^2 c_z}{\partial z^2} - k_{app} c_Z \quad (2)$$

Next, the mass balance equation of the same analyte in region y of the diffusion column, filled with the solid material under study:

$$\frac{\partial c_y}{\partial t} = D_2 \frac{\partial^2 c_y}{\partial y^2} - k_{-1} \frac{a_s}{a_y} (c_s^* - c_s) - k_{app} c_y \quad (3)$$

Finally, the rate of change of the adsorbed concentration:

$$\frac{\partial c_s}{\partial t} = k_{-1}(c_s^* - c_s) - k_2 c_s \quad (4)$$

with the symbols above denoting:

c_s^* equilibrium adsorbed concentration of the analyte at time t, mol g^{-1}.
m_s initially adsorbed equilibrium amount of this analyte, mol.
a_s amount of solid material per unit length of column bed, g cm^{-1}.
$\delta(y-L_2)$ Dirac's delta function for the initial condition of the bed, when the analyte is introduced as an instantaneous pulse at the point $y=L_2$, cm^{-1}.
y length coordinate along section L_2, cm.
a_y cross sectional area of the void space in region y, cm^2.
k_1 local adsorption parameter, s^{-1}.
c_y gaseous concentration of the analyte as a function of time t and coordinate y along the column, mol cm^{-3}.
τ dummy variable for time, s.
c_z gaseous concentration of the analyte as a function of time t and length coordinate z along the column, mol cm^{-3}.
D_1 diffusion coefficient of this analyte into the carrier gas (nitrogen), cm^2 s^{-1}.
k_{app} apparent rate constant of a first-order or pseudofirst-order reaction of the analyte in the gas phase, s^{-1}.
D_2 diffusion coefficient of this analyte into the carrier gas in section y, cm^2 s^{-1}.
k_{-1} rate constant for desorption of the analyte from the solid bulk, s^{-1}.
c_s concentration of the analyte adsorbed on the solid at time t, mol g^{-1}.
k_2 the rate constant of a possible first-order or pseudofirst-order surface reaction of the adsorbed analyte, s^{-1}.

It appears that the term $(c_s^* - c_s)$ in both Eqs. (3) and (4) describes a linear ''near equilibrium behavior'' isotherm, but this is not so, since, after taking the Laplace transforms of Eqs. (3) and (4), and eliminating the transformed function c_s between them, the no-model isotherm of Eq. (1) is also transformed and substituted for the transformed c_s^* function in the equation resulting from Eqs. (3) and (4) (for details see Ref. [12]). The final solution takes into account the initial conditions $c_y(0, y) = \frac{m}{a_y}\delta(y - L_2)$, and $c_s(0, y) = 0$, m being the amount (mol) of the analyte introduced as a pulse at $y = L_2$, and the linking with the solution of Eq. (2) at $z = L_1$ and $y = 0$. The final function obtained is [12]:

$$H^{1/M} = gc(l', t) = \sum_{i=1}^{4} A_i \exp(B_i t) \quad (5)$$

together with the values of the quantities k_1, k_{-1}, k_2, k_{app}, and D_1. In Eq. (5) the symbols denote:

H height of sample peaks resulting from the flow reversal, cm.
M response factor of the detector, dimensionless.
g calibration factor of the detector, cm/mol cm^{-3}.
$c(l', t)$ measured sampling concentration of the analyte at $x = l'$ or $z = 0$, mol cm^{-3}.

The explicit calculation of the isotherms for the hydrocarbons C_6H_6 and C_7H_8 in the presence of NO_2 can be carried out in an analogous way as that described earlier [5], when the calculation of g was also described. The isotherms refer to the values of $c_y(0, t)$, i.e., the gaseous concentration of the analyte at $y = 0$:

$$c_y(0, t) = \frac{vL_1}{D_1} c(l', t) = \frac{vL_1}{gD_1} \sum_{i=1}^{4} A_i \exp(B_i t) \quad (6)$$

where v is the linear velocity of the carrier gas (cm s^{-1}) in the sampling column and L_1 the length of the diffusion column (cm). From this, the value of c_s^* is calculated by means of Eq. (1) for $c_y(\tau)=c_y(0, \tau)$:

$$c_s^* = \frac{a_y}{a_s} k_1 \frac{vL_1}{gD_1} \sum_{i=1}^{4} \frac{A_i}{B_i} [\exp(B_i t) - 1] \quad (7)$$

Although c_s^* as calculated here refers only to the value $y=0$ of the length coordinate y, this does not mean one kind of adsorption site only, since a whole cross sectional area $a_y(1-\varepsilon)/\varepsilon$ (ε=external porosity) of the bed is filled with solid at anyone value of y. In this area of varying tube radius a wide range of adsorption sites is possible.

The differential isotherm is found from the obvious relation $\partial c_s^*/\partial c_y = (\partial c_s^*/\partial t)/(\partial c_y/\partial t) = (a_y/a_s)k_1 c_y(t)/(\partial c_y/\partial t)$:

$$\frac{\partial c_s^*}{\partial c_y} = \frac{a_y}{a_s} k_1 = \frac{\sum_{i=1}^{4} A_i \exp(B_i t)}{\sum_{i=1}^{4} A_i B_i \exp(B_i t)} \quad (8)$$

In all equations above A_i and B_i are the pre-exponential factors and the exponential coefficients of Eq. (5). One can use τ in the above equations as a dummy independent variable for the time t and calculate, for chosen arbitrary values of τ, all three variables c_y, c_s^* and $\partial c_s^*/\partial c_y$. Plotting $\partial c_s^*/\partial c_y$ or c_s^* against c_y for each chosen τ, independent experimental isotherms can be obtained.

4. Results and discussion

Usually in the studies of physical adsorption on heterogeneous surfaces, the following procedure is applied: the energy distribution function is evaluated from an overall adsorption isotherm given in an analytical or tabulated form, from experimental adsorption data [4]. Thus the existence of such a table is valuable for studying the surface energy distribution.

Here the simultaneous adsorption equilibrium of a binary gas mixture on a solid surface can be described by three variables: $\partial c_s^*/\partial c_y$, c_s^* and c_y. Thus, two types of isotherms are used for the description of adsorption equilibrium in this paper: the differential and the integrated one. Both are tabulated in Tables 2–6 (first and second column respectively) with the

Table 2
Sample isotherms for the adsorption of benzene and toluene on zinc oxide in the presence of NO_2 at 363.2 and 393.2 K, respectively

Dummy variable (min)	Benzene and nitrogen dioxide on zinc oxide			Toluene and nitrogen dioxide on zinc oxide		
	$(\partial c_s^*/\partial c_y)$ ($cm^3\ g^{-1}$)	c_s^* (10^{-6} mol g^{-1})	c_y (10^{-6} mol cm^{-3})	$(\partial c_s^*/\partial c_y)$ ($cm^3\ g^{-1}$)	c_s^* (10^{-5} mol g^{-1})	c_y (10^{-6} mol cm^{-3})
10	0.281	0.788	5.802	0.914	0.485	8.071
15	−2.154	1.435	6.484	−4.504	0.723	8.876
20	−0.657	2.067	5.792	−1.600	1.045	7.640
25	−0.570	2.611	4.880	−1.298	1.270	6.052
30	−0.587	3.068	4.085	−1.249	1.445	4.668
35	−0.646	3.451	3.459	−1.302	1.579	3.605
40	−0.736	3.779	2.982	−1.434	1.684	2.833
45	−0.852	4.064	2.620	−1.647	1.767	2.287
50	−0.996	4.317	2.345	−1.954	1.836	1.904
55	−1.168	4.545	2.133	−2.389	1.893	1.634
60	−1.366	4.754	1.968	−2.903	1.944	1.442
65	−1.584	4.948	1.835	−3.549	1.988	1.302
70	−1.815	5.130	1.728	−4.282	2.029	1.196
75	−2.049	5.301	1.639	−5.056	2.067	1.115
80	−2.276	5.465	1.564	−5.814	2.103	1.050
85	−2.486	5.621	1.498	−6.502	2.136	0.996
90	−2.675	5.771	1.440	−7.089	2.168	0.949

$k_1(C_6H_6)=6.530\cdot10^{-4}\ s^{-1}$, $k_1(C_7H_8)=2.096\cdot10^{-3}\ s^{-1}$.

Table 3
Sample isotherms for the adsorption of benzene and toluene on lead oxide in the presence of NO_2 at 363.2 and 393.2 K, respectively

Dummy variable (min)	Benzene and nitrogen dioxide on lead oxide			Toluene and nitrogen dioxide on lead oxide		
	$(\partial c_s^*/\partial c_y)$ ($cm^3\ g^{-1}$)	c_s^* (10^{-6} mol g^{-1})	c_y (10^{-6} mol cm^{-3})	$(\partial c_s^*/\partial c_y)$ ($cm^3\ g^{-1}$)	c_s^* (10^{-5} mol g^{-1})	c_y (10^{-6} mol cm^{-3})
10	0.193	0.611	8.585	0.0044	0.180	10.13
15	−10.50	1.238	9.850	0.212	0.477	13.59
20	−0.491	1.872	9.089	−0.398	0.815	13.80
25	−0.359	2.429	7.716	−0.163	1.135	12.37
30	−0.335	2.894	6.361	−0.124	1.412	10.38
35	−0.344	3.276	5.227	−0.110	1.641	8.411
40	−0.374	3.592	4.342	−0.104	1.824	6.694
45	−0.421	3.856	3.673	−0.104	1.969	5.297
50	−0.486	4.082	3.171	−0.108	2.084	4.207
55	−0.567	4.279	2.795	−0.115	2.176	3.377
60	−0.663	4.454	2.508	−0.126	2.250	2.756
65	−0.772	4.613	2.286	−0.142	2.311	2.296
70	−0.886	4.758	2.110	−0.164	2.363	1.957
75	−1.000	4.893	1.967	−0.193	2.407	1.706
80	−1.107	5.019	1.848	−0.231	2.446	1.520
85	−1.203	5.138	1.745	−0.279	2.482	1.381
90	−1.284	5.250	1.654	−0.336	2.514	1.275

$k_1(C_6H_6) = 1.820 \cdot 10^{-3}\ s^{-1}$, $k_1(C_7H_8) = 6.688 \cdot 10^{-4}\ s^{-1}$.

Table 4
Sample isotherms for the adsorption of benzene and toluene on iron oxide in the presence of NO_2 at 363.2 and 393.2 K, respectively

Dummy variable (min)	Benzene and nitrogen dioxide on iron oxide			Toluene and nitrogen dioxide on iron oxide		
	$(\partial c_s^*/\partial c_y)$ ($cm^3\ g^{-1}$)	c_s^* (10^{-6} mol g^{-1})	c_y (10^{-6} mol cm^{-3})	$(\partial c_s^*/\partial c_y)$ ($cm^3\ g^{-1}$)	c_s^* (10^{-5} mol g^{-1})	c_y (10^{-6} mol cm^{-3})
10	0.771	0.616	4.586	0.161	0.124	5.508
15	8.028	0.856	5.890	0.718	0.257	9.558
20	−5.110	1.114	5.725	−7.674	0.430	10.43
25	−3.309	1.354	5.106	−1.264	0.600	9.580
30	−3.064	1.564	4.438	−0.906	0.751	8.134
35	−3.190	1.746	3.852	−0.807	0.876	6.659
40	−3.517	1.905	3.375	−0.790	0.977	5.381
45	−3.999	2.045	3.000	−0.817	1.059	4.356
50	−4.614	2.170	2.707	−0.882	1.126	3.566
55	−5.341	2.284	2.477	−0.983	1.181	2.972
60	−6.148	2.389	2.294	−1.127	1.227	2.530
65	−6.996	2.487	2.145	−1.318	1.267	2.201
70	−7.838	2.579	2.021	−1.560	1.302	1.956
75	−8.632	2.666	1.916	−1.855	1.334	1.770
80	−9.344	2.748	1.824	−2.196	1.362	1.516
85	−9.956	2.826	1.743	−2.570	1.389	1.426
90	−10.46	2.902	1.699	−2.958	1.414	1.351

$k_1(C_6H_6) = 2.441 \cdot 10^{-3}\ s^{-1}$, $k_1(C_7H_8) = 9.375 \cdot 10^{-4}\ s^{-1}$.

Table 5
Sample isotherms for the adsorption of benzene and toluene on titanium oxide in the presence of NO_2 at 363.2 and 393.2 K, respectively

Dummy variable (min)	Benzene and nitrogen dioxide on titanium oxide			Toluene and nitrogen dioxide on titanium oxide		
	$(\partial c_s^*/\partial c_y)$ ($cm^3\ g^{-1}$)	c_s^* (10^{-6} mol g^{-1})	c_y (10^{-6} mol cm^{-3})	$(\partial c_s^*/\partial c_y)$ ($cm^3\ g^{-1}$)	c_s^* (10^{-5} mol g^{-1})	c_y (10^{-6} mol cm^{-3})
10	0.205	0.398	1.042	0.245	0.469	1.266
15	0.920	0.514	3.447	1.002	0.723	5.585
20	3.756	0.724	4.671	2.707	1.274	8.936
25	−23.30	0.968	4.885	9.968	2.009	10.52
30	−5.830	1.208	4.606	−23.04	2.806	10.69
35	−4.585	1.429	4.166	−7.859	3.580	10.00
40	−4.465	1.627	3.723	−5.659	4.286	8.923
45	−4.753	1.805	3.336	−4.905	4.906	7.735
50	−5.286	1.964	3.016	−4.644	5.440	6.612
55	−5.997	2.109	2.758	−4.644	5.894	5.630
60	−6.832	2.243	2.549	−4.828	6.282	4.808
65	−7.734	2.367	2.378	−5.170	6.614	4.141
70	−8.643	2.483	2.236	−5.664	6.902	3.608
75	−9.502	2.592	2.116	−6.305	7.154	3.185
80	−10.27	2.696	2.011	−7.085	7.378	2.848
85	−10.93	2.795	1.918	−7.986	7.764	2.580
90	−11.46	2.889	1.833	−8.977	7.933	2.363

$k_1(C_6H_6) = 1.994 \cdot 10^{-3}\ s^{-1}$, $k_1(C_7H_8) = 2.948 \cdot 10^{-3}\ s^{-1}$.

Table 6
Sample isotherms for the adsorption of benzene and toluene on chromium oxide in the presence of NO_2 at 363.2 and 393.2 K, respectively

Dummy variable (min)	Benzene and nitrogen dioxide on chromium oxide			Toluene and nitrogen dioxide on chromium oxide		
	$(\partial c_s^*/\partial c_y)$ ($cm^3\ g^{-1}$)	c_s^* (10^{-6} mol g^{-1})	c_y (10^{-6} mol cm^{-3})	$(\partial c_s^*/\partial c_y)$ ($cm^3\ g^{-1}$)	c_s^* (10^{-5} mol g^{-1})	c_y (10^{-6} mol cm^{-3})
10	0.212	1.056	1.662	0.114	0.466	3.458
15	0.757	1.687	3.214	0.450	0.538	6.548
20	3.338	2.590	3.858	1.740	0.640	7.815
25	−8.510	3.574	3.920	−7.605	0.752	8.014
30	−3.282	4.533	3.706	−1.998	0.862	7.648
35	−2.612	5.424	3.394	−1.413	0.964	7.019
40	−2.482	6.235	3.073	−1.216	1.058	6.302
45	−2.560	6.969	2.781	−1.139	1.141	5.592
50	−2.763	7.634	2.530	−1.120	1.214	4.940
55	−3.062	8.241	2.320	−1.138	1.279	4.363
60	−3.442	8.801	2.148	−1.184	1.337	3.867
65	−3.885	9.321	2.005	−1.254	1.388	3.447
70	−4.369	9.808	1.887	−1.348	1.433	3.095
75	−4.866	10.27	1.787	−1.464	1.474	2.802
80	−5.350	10.71	1.701	−1.602	1.512	2.557
85	−5.796	11.12	1.626	−1.760	1.546	2.353
90	−6.188	11.52	1.560	−1.935	1.578	2.181

$k_1(C_6H_6) = 1.493 \cdot 10^{-3}\ s^{-1}$, $k_1(C_7H_8) = 8.323 \cdot 10^{-4}\ s^{-1}$.

corresponding values of c_y. From Tables 2–6, it is seen that the adsorbed amount c_s^* is not a unique function of the gas phase concentration c_y, as expected from an ordinary conventional adsorption isotherm. It seems as if a single partial pressure corresponding to c_y, can produce two different surface coverages at some areas. This behaviour stems from the fact that Eq. (1) does not give the total monolayer coverage of the entire homogeneous surface, but is a local adsorption equation for a heterogeneous surface, sweeping it over the various active sites of different adsorption energy with time. It is a usual experimental finding for c_y to increase with time initially, pass over a maximum and then decrease exponentially with time. Two different times may exhibit the same value for c_y, one in the ascending branch and the other in the descending one. But these do not correspond to the same value for the adsorbed concentration c_s^*, since different kinds of adsorption sites contribute to the adsorption process in the two above cases, i.e., at two different times. It follows that isotherm graphs similar to the conventional ones can be obtained by plotting c_s^* as a function of time. Figs. 3–5 give some examples. It is the author's opinion that these plots represent the behavior of the bulk adsorption material.

In Figs. 3–5 the pure-aromatic isotherms as well as the binary aromatic hydrocarbon–nitrogen dioxide ones on the same oxides are presented. The only experimental difference between pure aromatics and binary adsorptions is the presence of nitrogen dioxide in the latter ($v_{\text{hydrocarbon}}/v_{NO_2} = 20$).

In six systems: C_6H_6–NO_2–PbO, C_6H_6–NO_2–TiO_2, C_6H_6–NO_2–Fe_2O_3, C_7H_8–NO_2–TiO_2, C_7H_8–NO_2–ZnO and C_7H_8–NO_2–Cr_2O_3, a displacement to higher adsorption values, as compared with the respective pure aromatic compounds, is noted, under the same experimental conditions. In three other cases: C_7H_8–NO_2–Fe_2O_3, C_6H_6–NO_2–ZnO, C_6H_6–NO_2–Cr_2O_3 the displacement is opposite, i.e., to lower values. Finally, the systems: C_7H_8–NO_2–PbO and C_7H_8–PbO show about the same adsorption isotherms.

Among TiO_2, Fe_2O_3, Cr_2O_3, ZnO and PbO studied with benzene or toluene in the presence of nitrogen dioxide, the isotherm of the last oxide with benzene has the smallest values of c_s^*, while the TiO_2 has the highest. The shape of the isotherms

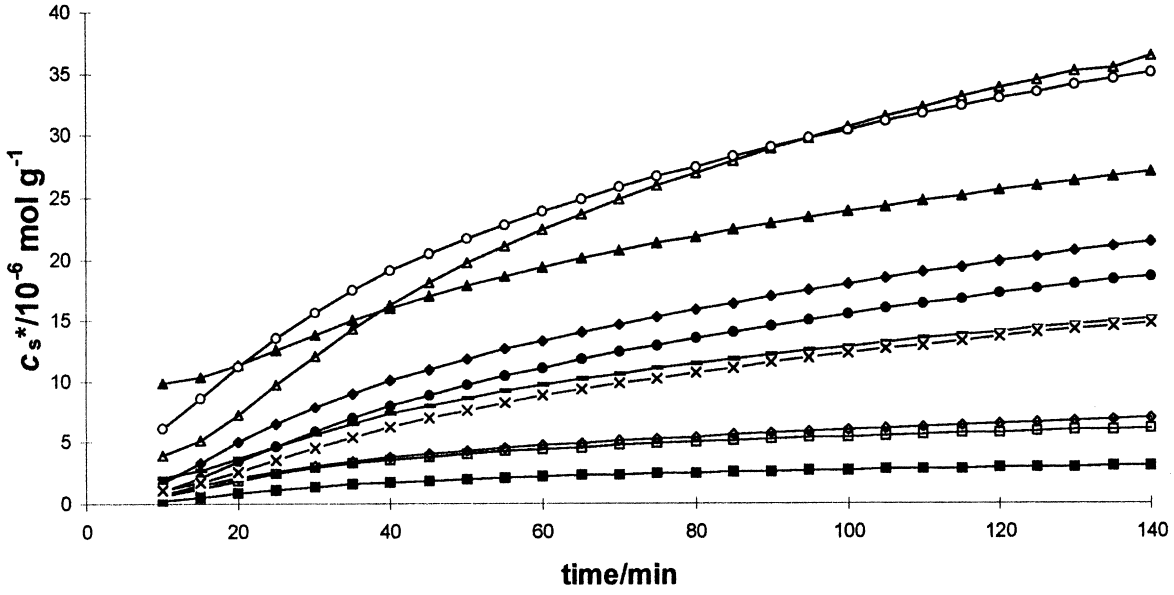

Fig. 3. Adsorption isotherms (in nitrogen atmosphere) of pure benzene and of benzene–nitrogen dioxide, on five solids as follows: (◇) C_6H_6–NO_2–ZnO; (♦) C_6H_6–ZnO; (×) C_6H_6–NO_2–Cr_2O_3; (—) C_6H_6–Cr_2O_3; (□) C_6H_6–NO_2–PbO; (■) C_6H_6–PbO; (△) C_6H_6–NO_2–TiO_2; (▲) C_6H_6–TiO_2; (○) C_6H_6–NO_2–Fe_2O_3; (●) C_6H_6–Fe_2O_3.

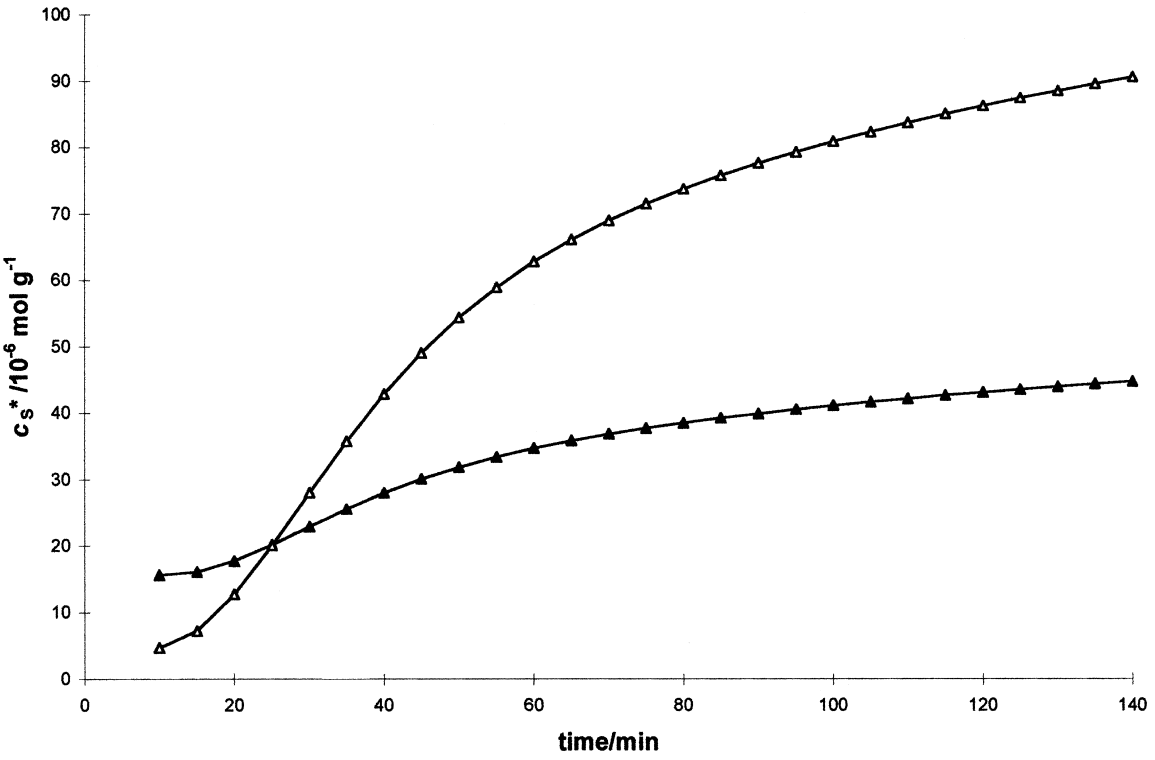

Fig. 4. Adsorption isotherms (in nitrogen atmosphere) of pure toluene (▲) and of toluene–nitrogen dioxide (△) on TiO_2.

remain always unchanged. The maximum value for c_y corresponding to a certain c_s^* may be due to a completion of a monolayer of adsorbed molecules. Further increase of c_s^* can be interpreted as due to multilayer adsorption, causing a decrease in c_y [5]. All the above lead to very different values of the physicochemical constants determined, among which the deposition velocity and the reaction probability are the highest [11–13].

It is believed that the present method offers a simple way to draw safe and accurate conclusions about chemical reactivity of many systems, which can be examined with the same method based on the experimentally obtained isotherms.

The present method gives accurate values of the kinetic constants k_1, k_{-1} and k_2 [12,13], in addition to the nonlinear model isotherm calculation, with a suitable personal computer program. Heterogeneity of the surface, like that of the oxides studied here, would not permit a linear adsorption isotherm model.

4.1. Comparison with other methods

A complete statistical description of real multicomponent adsorption systems is still a unsolved problem. Thus, applications of this treatment for characterization of real adsorption systems and prediction of adsorption from multicomponent mixtures is impossible at present; in addition, the further complication introduced through the heterogeneity of the surface makes a full statistical thermodynamical treatment untenable [4].

Of the classical methods for measuring adsorption, only volumetric methods have been used to measure binary adsorption equilibrium [16]. These methods lack the speed precision and temperature range of the RF-GC method.

When using the elution method (the best one among the older GC methods) to obtain the adsorption isotherms, the sorption effect, that is to say, the change in gas flow-rate caused by the sorption or

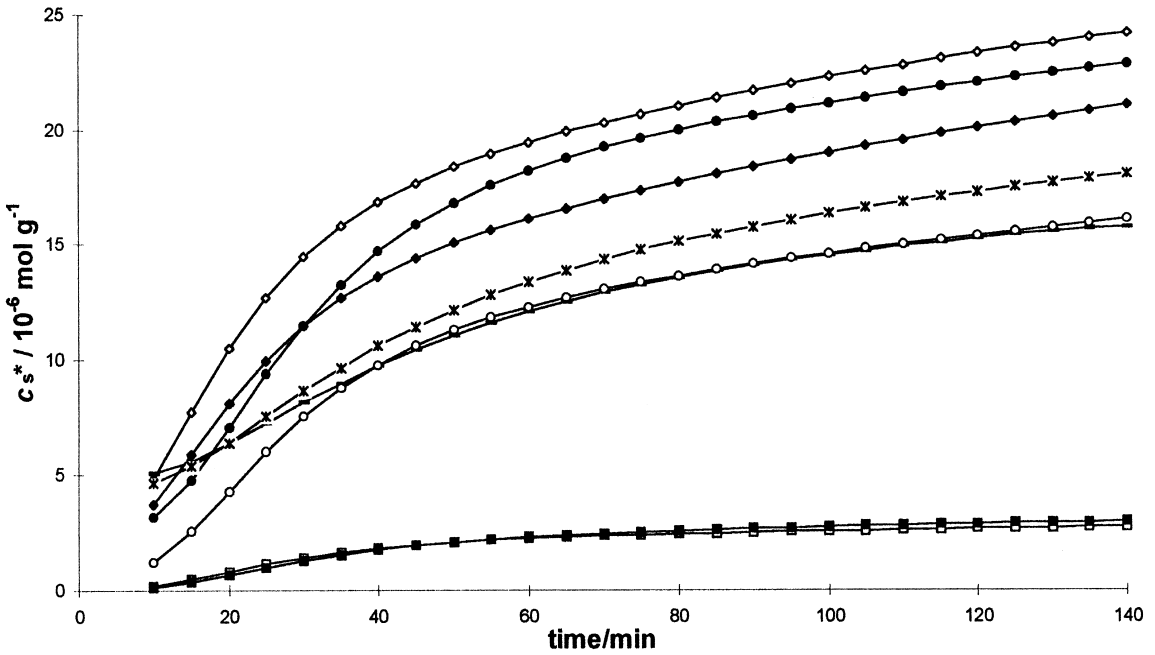

Fig. 5. Adsorption isotherms (in nitrogen atmosphere) of pure toluene and of toluene–nitrogen dioxide on four solids as follows: (◇) C_7H_8–NO_2–ZnO; (♦) C_7H_8–ZnO; (×) C_7H_8–NO_2–Cr_2O_3; (—) C_7H_8–Cr_2O_3; (□) C_7H_8–NO_2–PbO; (■) C_7H_8–PbO; (○) C_7H_8–NO_2–Fe_2O_3; (●) C_7H_8–Fe_2O_3.

desorption of the solute molecules in the stationary phase causes the greatest error in the isotherm determination [15–17].

In the RF-GC method the sorption effect is nonexistent. Besides this method has the following advantages: (1) the diffusion and resistance to mass transfer are not neglected; (2) pressure gradient is negligible along the bed; (3) it leads directly to an experimental isotherm without specifying a priori an isotherm equation; (4) the isotherm can be determined in the presence of a surface reaction of the adsorbate; (5) it is simple and fast; (6) it has an acceptable accuracy [5,12,13].

5. Conclusions

Adsorption of mixtures of gases and vapors on solids is of significant interest in many diverse areas of chemistry. Various forms of perturbation chromatography have been used to measure pure-component isotherms and in few cases even binary isotherms. In this work, a systematic study of two binary systems, C_6H_6–NO_2 and $C_6H_5CH_3$–NO_2, on five adsorbents is presented. The technique used is RF-GC, a known perturbation chromatographic one, with many advantages. Determination of these binary isotherms on well-characterized adsorbents will provide the data base needed for the development of the models to analyze and interpret such data.

Acknowledgements

Support of this work by the European Commission with the contract EV5V-CT94-0537 is gratefully acknowledged.

References

[1] M. Domingo-Garcia, F.J. Lopez-Garzon, R. Lopez-Garzon, C. Moreno-Castilla, J. Chromatogr. 324 (1985) 19.
[2] J. Jaroniec, Phys. Lett. 59A (1976) 259.
[3] J. Roles, G. Guiochon, J. Chromatogr. 591 (1992) 233.

[4] M. Jaroniec, R. Madey, Physical Adsorption on Heterogeneous Solids, Elsevier, Oxford, New York, 1988.
[5] V. Sotiropoulou, G.P. Vassilev, N.A. Katsanos, H. Metaxa, F. Roubani-Kalantzopoulou, J. Chem. Soc., Faraday Trans. 91 (1995) 485.
[6] J.F. Parcher, K.J. Hyver, J. Chromatogr. 302 (1984) 195.
[7] N.A. Katsanos, J. Chem. Soc., Faraday Trans. 1 78 (1982) 1051.
[8] N.A. Katsanos, Flow Pertubation Gas Chromatography, Marcel Dekker, New York, Basel, 1988, pp. 87-111.
[9] V. Sotiropoulou, N.A. Katsanos, H. Metaxa, F. Roubani-Kalantzopoulou, Chromatographia 42 (1996) 441.
[10] F. Roubani-Kalantzopoulou, E. Kalogirou, A. Kalantzopoulos, H. Metaxa, R. Thede, N.A. Katsanos, V. Sotiropoulou, Chromatographia 46 (1997) 161.
[11] G. Karagiorgos, F. Roubani-Kalantzopoulou, Z. Phys. Chem. 203 (1998) 231.
[12] Ch. Abatzoglou, E. Iliopoulou, N.A. Katsanos, F. Roubani-Kalantzopoulou, A. Kalantzopoulos, J. Chromatogr. A 775 (1997) 211.
[13] H. Zahariou-Rakanta, A. Kalantzopoulos, F. Roubani-Kalantzopoulou, J. Chromatogr. A 776 (1997) 275.
[14] X. Yun, Z. Long, D. Kou, X. Lu, H. Li, J. Chromatogr. A 736 (1996) 151.
[15] N.A. Katsanos, R. Thede, F. Roubani-Kalantzopoulou, J. Chromatogr. A 795 (1998) 133.
[16] E. Van der Vlist, J. Van der Meijden, J. Chromatogr. 79 (1973) 1.
[17] R.G. Gerritse, J.F.K. Huber, J. Chromatogr. 71 (1972) 173.